Journal Pre-proof

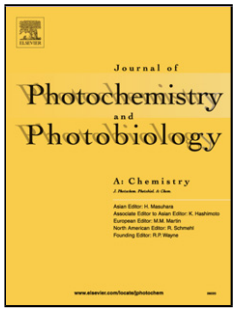

Barbiturate squaraine dyes as fluorescent probes for serum albumins detection

Vanessa S.D. Gomes, Helena M.R. Gonçalves, Renato E.F. Boto, Paulo Almeida, Lucinda V. Reis

PII: S1010-6030(20)30509-8

DOI: https://doi.org/10.1016/j.jphotochem.2020.112710

Reference: JPC 112710

To appear in: *Journal of Photochemistry & Photobiology, A: Chemistry*

Received Date: 30 March 2020

Revised Date: 12 June 2020

Accepted Date: 13 June 2020

Please cite this article as: Gomes VSD, Gonçalves HMR, Boto REF, Almeida P, Reis LV, Barbiturate squaraine dyes as fluorescent probes for serum albumins detection, *Journal of Photochemistry and amp; Photobiology, A: Chemistry* (2020), doi: https://doi.org/10.1016/j.jphotochem.2020.112710

Barbiturate squaraine dyes as fluorescent probes for serum albumins detection

Vanessa S. D. Gomes[1], Helena M.R. Gonçalves[1,2], Renato E. F. Boto[3,4], Paulo Almeida[3,4], Lucinda V. Reis[1,5*]

[1]Chemistry Centre of Vila Real (CQ-VR), University of Trás-os-Montes and Alto Douro, Quinta de Prados, 5001-801, Vila Real, Portugal;
[2]REQUIMTE, Instituto Superior de Engenharia do Porto, 4200-072 Porto, Portugal;
[3]Health Sciences Research Centre (CICS-UBI), University of Beira Interior, Av. Infante D. Henrique, 6201-506 Covilhã, Portugal
[4]Chemistry Department, University of Beira Interior, Rua Marquês d'Ávila e Bolama, 6201-001, Covilhã, Portugal
[5]Chemistry Department, University of Trás-os-Montes and Alto Douro, Quinta de Prados, 5001-801, Vila Real, Portugal

***** Chemistry Department and CQ-VR; School of Life and Environmental Sciences, University of Trás-os-Montes e Alto Douro (UTAD); Quinta de Prados; 5001-801 Vila Real; Portugal.
Tel.: +351 259350225; Fax: +351 29350480; E-mail address: lucinda.reis@utad.pt

Highlights

- Three squaraine cyanine dyes possessing in their structures moieties derived from barbituric acid was synthesized and fully characterized.
- The potential as probes for HSA and BSA detection of the three squaraine cyanine dyes was studied.
- The binding constants showed that the dyes have a strong interaction and high affinity for both proteins.
- The Zeta potential values revealed that the dyes are quite stable in aqueous media.

Abstract

Three indolenine-based barbiturate squaraine dyes were synthesized, characterized and subjected to photophysical studies, including their affinity with human serum albumin and bovine serum albumin as protein models in phosphate buffer solution. All dyes successfully interact with both proteins with high affinity binding constants. It was found that dyes with hydrophobic substituents had superior binding constants with both proteins. The fluorescence intensity of all dyes increased in the presence of both proteins which allowed the determination of detection and quantifications limits in the tens of nanomolar, using a protein concentration of 0 – 3.5 μM. Concerning to the study on the binding sites of the synthesized dyes using the warfarin and ibuprofen markers, the results of this study suggest that, one dye binds to both BSA binding sites while the two others dyes binds only to site I, and that all three dyes bind to both HSA binding sites.

Keywords: Barbiturate, Squaraine dyes, Near-IR-emitting, Fluorescent probes, Serum albumins

---

1. Introduction

In the biomedical diagnosis area, the determination of serum albumin (SA) concentration is a fundamental parameter to assess the patient's health. It provides a secure prognosis for development of some diseases in both healthy and apparently healthy individuals [1]. SA like human serum albumin (HSA) and bovine serum albumin (BSA) are a family of water-soluble globular proteins, within which SA is the major protein in blood plasma. Over the years has been the most studied class of proteins due to their properties, such as stability and ability to bind and transport several ligands to specific sites [2, 3]. Albumins have an essential role in the maintenance of various metabolic processes, such as, determining plasma oncotic pressure, antagonizing the activity of toxins and controlling the anti-oxidant properties of plasma, among others [4-7]. Therefore, changes in albumin concentration can be used as early stage biomarker for several disorders, such as cardiovascular disease, liver injury, glomerular failure, diabetes, among others [8, 9]. Given its relevance in biological systems, its quantitative determination in fluids is of great importance in clinical diagnosis. Nowadays there are several detection methods in used, namely colorimetric techniques (Lowry and Bradford method), immunoassays,

Surface-Enhanced Raman Scattering (SERS), cyclic voltammetry and chemiluminescence. However, these techniques have several drawbacks, the main one being the need of specific equipment and specialized personnel, which increases the cost efficiency of the processes, along with difficult sample preparation protocols [10-12].

The search for new methods that may overcome these disadvantages and allow rapid, low-cost and non-invasive assessment is a constantly developing area. One of the appealing alternatives is the fluorescence spectroscopy. This technique is a powerful tool that offers unique advantages, e.g, simplicity, excellent sensitivity and compatibility with both live cells and physiological assays and cost efficiency [13, 14]. Several fluorescence-based methods are being developed especially in the clinical and biological research areas [15, 16].

Polymethine dyes are a class of compounds that have unique properties, namely, sharp and intense absorption in the red-near infrared (NIR) region, high extinction coefficient, intense fluorescence and moderate photoconductivity [17, 18]. These characteristics make them a target of interest for both technological and biological applications, particularly as organic solar cell sensitizers [19, 20], photoconductive materials [21, 22], photodynamic therapy photosensitizers [23, 24], as well as fluorescent probes and labels [25-28]. Some squaraine dyes features a two-photon excited fluorescence effect (TPEF), what makes them very appealing for use in bioimaging because it allows to obtain deeper and clearer images [29].

Here it is presented for the first time the synthesis of two innovative squaraine dyes with a barbiturate group that were successfully used for SA fluorescence detection. We also used the dye **8a** previously reported by some of us [23], which had not yet been used in this type of tests. The binding mechanism that BSA and HSA have in the presence of increasing amounts of the three dyes were fully explored. Moreover, since the fluorescence enhancement provided by the formation of the dye-protein complex was linear and, as such, it was possible to determine the system detection limit (DL), quantification limit (QL) and sensitivity.

2. Materials and Methods

Chemicals and reagents (e.g. 2,3,3-trimethylindolenine (**1**), 3,4-dihydroxycyclobut-3-en-1,2-dione, barbituric acid (**6a**), thiobarbituric acid (**6b**), BSA, HSA, warfarin and ibuprofen, were purchased from commercial suppliers and used without further

purification unless otherwise noted. 1-Hexyl-2,3,3-trimethylindolin-1-ium iodide (**2**) [30], 3,4-dibutoxycyclobut-3-en-1,2-dione (**4**) [31], 3-butoxy-4-[(1-hexyl-3,3-dimethylindol-3H-ylidene)methyl]-cyclobut-3-en-1,2-dione (**5**) [23], 1,3‑diphenylthiourea (**6c$_3$**) [32], 1,3-diphenyl-2-thiobarbituric acid (**6c$_5$**) [32], triethylammonium 2-[(1-hexyl-3,3-dimethylindolin-2-ylidene)methyl]-4-oxo-3-(2,4,6-trioxohexahydro-5-pyrimidinyliden)cyclobut-1-en-1-olate (**7a**) [23] and 4-[(1-hexyl-3,3-dimethyl-3H-indol-1-ium-2-yl)methylidene]-2-[(1-hexyl-3,3-dimethylindolin-2-ylidene)methyl]-3-(2,4,6-trioxohexahydro-5-pyrimidinyliden)cyclobut-1-en-1-olate (**8a**) [23] were prepared according to the literature procedure.

All reactions were monitored by thin-layer chromatography (TLC) on aluminium plates with 0.25 mm of silica gel (Merck 60 F254). Melting points (m.p.) were measured in a hot plate binocular microscope apparatus (URA Technic, Portugal) and were uncorrected. Visible (Vis) spectra were obtained on a Perkin Elmer Lambda 25 instrument; λ_{max} in nanometers (nm). The infrared (IR) spectra were recorded on a UNICAM Research Series FTIR spectrophotometer using KBr pellets; υ_{max} in cm^{-1}. The bands were described as s (strong), m (medium) or w (weak). Nuclear magnetic resonance of proton (^{1}H NMR) and nuclear magnetic resonance of carbon-13 (^{13}C NMR) spectra were obtained at 298.15 K on a NMR Brucker Avance III 400 spectrometer operating at 9.4 T, observing ^{1}H at 400.13 MHz and ^{13}C at 100.62 MHz. The solutions were prepared in $CDCl_3$ and the chemical shifts are expressed as δ (ppm) relative to tetramethylsilane (internal standard) or to residual solvent signals and the coupling constant (J) values are given in hertz (Hz). Splittings were described as s (singlet), d (doublet), t (triplet), qt (quintet) or combinations of the above or m (multiplet). Chemical shifts of ^{13}C NMR spectra are presented to the hundredths because after rounding to the tenths the signals of some different carbons would appear to the same chemical shift. The assignments of the carbon were made based on Distortionless Enhancement by Polarization Transfer (DEPT 135) spectra. High resolution electrospray ionization time-of-flight mass spectra (HRESI-TOFMS) were

recorded using a microTOF (focus) Brucker Daltonics spectrometer (C.A.C.T.I. at the University of Vigo).

2.1. Synthesis and characterization of precursors and squaraine dyes

*2.1.1. Synthesis of triethylammonium 2-[(1-hexyl-3,3-dimethylindolin-2-ylidene)methyl]-4-oxo-3-(4,6-dioxo-2-thioxohexahydro-5-pyrimidinyliden)cyclobut-1-en-1-olate (**7b**)*

The title compound was prepared by a similar method described by Tatarets *et al.* [33], from a reaction of the semisquaraine **5** (1.084 g, 2.74 mmol) and thiobarbituric acid (**6b**) (0.593 g, 4.11 mmol) in ethanol (20 mL) in the presence of triethylamine (0.380 mL, 2.74 mmol). The mixture was stirred under reflux for 6 h and then was cooled on an ice bath to allow the product to precipitate by the addition of diethyl ether. The resulting residue was washed with heated diethyl ether, filtered under reduced pressure and used in the next step without further purification.

*2.1.2. Synthesis of triethylammonium 2-[(1-hexyl-3,3-dimethylindolin-2-ylidene)methyl]-4-oxo-3-(4,6-dioxo-1,3-diphenyl-2-thioxotetrahydro-5-pyrimidinyliden)cyclobut-1-en-1-olate (**7c**)*

The title compound was synthetized analogously to **7b**, from a reaction of the semisquaraine **5** (0.585 g, 1.48 mmol) and compound **6c**$_5$ (0.657 g, 2.22 mmol) in ethanol (15 mL) in the presence of triethylamine (0.205 mL, 1.48 mmol). The mixture was stirred under reflux for 7 h and then was cooled on an ice bath to allow the product to precipitate by the addition of diethyl ether. The resulting residue was washed with heated diethyl ether, filtered under reduced pressure and used in the next step without further purification.

*2.1.3. Synthesis of 3-(4,6-dioxo-2-thioxotetrahydro-5-pyrimidinyliden)-4-[(1-hexyl-3,3-dimethyl-3H-indol-1-ium-2-yl)methylidene]-2-[(1-hexyl-3,3-dimethylindolin-2-ylidene)methyl]cyclobut-1-en-1-olate (**8b**)*

The title dye was prepared by reaction of the semisquaraine dye **7b** (0.92 g, 1.62 mmol) with the ammonium quaternary salt **2** (0.60 g, 1.62 mmol) in a mixture (1:1 v/v) of *n*-butanol/toluene (20 mL), stirred for 8 h at reflux in a Dean-Stark apparatus. The reaction mixture was quenched with cold distilled water, and the organic layer, after separation by decantation, dried with anhydrous Na_2SO_4 and the solvent removed under reduced

pressure. The obtained residue was purified by successive recrystallizations from CH_2Cl_2/ petroleum ether/ diethyl ether. Dark green crystals were recoiled and dried under reduced pressure. Yield: 5%; m.p.: 259-260 ºC; Vis λ_{max} (DMF): 652 nm, log ε = 5.17; Vis λ_{max} (PBS): 645 nm; IR υ_{max} (KBr): 3420 (w, NH), 3067 (w, ArCH), 2955 (m, CH), 2926 (m, CH), 2857 (m, CH), 1740 (m, C=O), 1597 (m, ArC=C), 1493 (s), 1454 (s), 1358 (m), 1288 (s), 1236 (w), 1219 (w), 1175 (m), 1153 (m), 1109 (s), 1057 (m), 1018 (w), 980 (w), 922 (m), 820 (w), 789 (w), 748 (w), 687 (w); ^{1}H NMR (400.13 MHz, $CDCl_3$) δ: 8.77 (2H, s, NH, exchange with D_2O), 7.38-7.34 (4H, m, ArH), 7.22 (2H, t, J = 7.4, ArH), 7.07 (2H, d, J = 7.6, ArH), 6.29 (2H, s, C<u>H</u>=C), 4.00 (4H, t, J = 7.4, NC<u>H</u>$_2$(CH$_2$)$_4$CH$_3$), 1.82 (4H, qt, NCH$_2$C<u>H</u>$_2$(CH$_2$)$_3$CH$_3$), 1.75 (12H, s, C(C<u>H</u>$_3$)$_2$), 1.43 (4H, qt, N(CH$_2$)$_2$C<u>H</u>$_2$(CH$_2$)$_2$CH$_3$), 1.38-1.31 (8H, m, N(CH$_2$)$_3$(C<u>H</u>$_2$)$_2$CH$_3$), 0.91 (6H, t, J = 6.8, N(CH$_2$)$_5$C<u>H</u>$_3$); ^{13}C NMR (100.6 MHz, $CDCl_3$) δ: 180.37, 174.91, 173.95, 173.01, 172.79, 160.62, 142.54, 141.86, 128.04 (ArCH), 124.85 (ArCH), 122.26 (ArCH), 110.37 (ArCH), 93.73 (<u>C</u>H=C), 88.41, 49.51 (<u>C</u>(CH$_3$)$_2$), 44.77 (N<u>C</u>H$_2$), 31.30 (CH$_2$), 26.86 (CH$_2$), 26.63 (CH$_2$), 26.42 (C(<u>C</u>H$_3$)$_2$), 22.49 (CH$_2$), 14.01 (CH$_3$); HRESI-TOFMS m/z: 690.3598 $[M]^+$ ($C_{42}H_{50}N_4O_3S$ calc. 690.3606).

*2.1.4. Synthesis of 3-(4,6-dioxo-1,3-diphenyl-2-thioxotetrahydro-5-pyrimidinyliden)-4-[(1-hexyl-3,3-dimethyl-3H-indol-1-ium-2-yl)methylidene]-2-[(1-hexyl-3,3-dimethylindolin-2-ylidene)methyl]cyclobut-1-en-1-olate (**8c**)*

The title dye was prepared by the reaction of the semisquaraine dye **5c** (0.240 g, 0.334 mmol) with the ammonium quaternary salt **2** (0.126 g, 0.334 mmol) in a mixture (1:1 v/v) of *n*-butanol/toluene (10 mL), stirred for 2 h at reflux in a Dean-Stark apparatus. After work-up in the same way as barbiturate squaraine dye **8b**, the obtained residue was purified by alumina column chromatography (CH_2Cl_2/MeOH, 2%). We obtained dark green crystals. Yield: 12%; M.p.: 250-251 ºC (dec.); Vis λ_{max} (DMF): 647 nm, log ε = 5.16; Vis λ_{max} (PBS): 650 nm; IR υ_{max} (KBr): 3057 (w, ArCH), 2957 (w, CH), 2927 (m, CH), 2860 (w, CH), 1741 (m, C=O), 1624 (m, ArC=C), 1491 (s), 1481 (s), 1454 (s), 1359 (s), 1290 (s), 1223 (w), 1179 (w), 1154 (w), 1129 (w), 1103 (m), 1054 (w), 1021 (w), 978 (w), 923 (w), 817 (w), 784 (w), 747 (w), 722 (w), 690 (w); ^{1}H NMR (400.13 MHz, $CDCl_3$) δ: 7.46 (4H, t, J = 7.4, ArH), 7.39-7.31 (10H, m, ArH), 7.19 (2H, t, J = 7.4, ArH), 7.0 (2H, d, J = 8.0, ArH), 6.32 (2H, s, <u>C</u>H=C), 3.86 (4H, t, J = 7.6, NC<u>H</u>$_2$(CH$_2$)$_4$CH$_3$), 1.73 (16H, br s,+ NCH$_2$C<u>H</u>$_2$(CH$_2$)$_3$CH$_3$), 1.34-1.27 (12H, m, N(CH$_2$)$_2$(C<u>H</u>$_2$)$_3$CH$_3$), 0.91 (6H, t, J =

6.6, $N(CH_2)_5C\underline{H}_3$); ^{13}C NMR (100.6 MHz, $CDCl_3$) δ: 180.65, 180.41, 175.60, 173.66, 172.69, 160.84, 142.86, 142.14, 141.86, 129.41 (ArCH), 129.22 (ArCH), 128.27 (ArCH), 128.00 (ArCH), 124.98 (ArCH), 122.52 (ArCH), 110.45 (ArCH), 94.45 ($\underline{C}H$=C), 90.27, 49.63 ($\underline{C}(CH_3)_2$), 45.03 ($N\underline{C}H_2$), 31.70 (CH_2), 27.16 (CH_2), 26.93 (CH_2), 26.69 ($C(\underline{C}H_3)_2$), 22.73 (CH_2), 14.38 (CH_3); HRESI-TOFMS m/z: 843.4302 $[M+H]^+$ ($C_{54}H_{59}N_4O_3S$ calc. 843.4285).

2.2. Preparation of dyes and protein solutions

The solutions were prepared by dissolution of dyes in dimethylformamide (DMF) to obtain a stock solution with a concentration of 6.7×10^{-4}M. The stock solutions of BSA and HSA with a concentration of 14 µM were prepared in PBS (0.05M, pH 7.2). In order to investigate protein/dye interactions, the DMF solutions of the dyes were diluted in PBS to have a concentration of 2 µM of each dye and then was added different volumes of BSA and HSA solutions to achieve the desired protein concentrations. All working solutions were prepared immediately before the assays.

2.3. Spectroscopic measurements

The absorption spectra of dyes were recorded on a Lambda 25 UV/Vis spectrophotometers (Perkin Elmer, USA) at room temperature (r.t.), using a spectral range between 500-900 nm. The emission spectra were obtained on a Varian Cary Eclipse fluorescence spectrophotometer (Agilent Technologies, USA). Spectroscopic measurements were performed in a standard quartz cell (1 cm path length).

2.4. Determination of fluorescence quantum yield

The fluorescence quantum yield was determined according to the equation 1 [34]:

$$\Phi_{dye} = \Phi_{ref}\left(\frac{Grad_{dye}}{Grad_{ref}}\right)\left(\frac{\eta^2_{dye}}{\eta^2_{ref}}\right) \qquad (1)$$

where the subscripts *ref* and *dye* denote reference and studied dyes respectively, *Grad* the gradient from the plot integrated fluorescence intensity *vs* absorbance and η the refractive index of the solvent (DMF). The reference used was zinc phthalocyanine (ϕ_F = 17% in DMF) [35]. The emission spectra were obtained with excitation wavelength λ_{exc}= 600 nm, excitation slit of 5 nm and emission slit of 10 nm.

2.5 Estimation of the dipole moments

The estimation of the ratio between the ground state and the excited state dipole moments (μg and μe, respectively) was calculated using the solvatochromic method according to the equations 2 and 3 [36].

$$\boldsymbol{va - vf = m_1 f(\varepsilon, n) + constant} \quad (2)$$

$$\boldsymbol{va + vf = -m_2 f(\varepsilon, n) + 2g(n) + constant} \quad (3)$$

where $\boldsymbol{va}$ and $\boldsymbol{vf}$ represent the absorption and fluorescence band shifts in different solvents that have a specific permittivity ($\boldsymbol{\varepsilon}$) and refractive index ($\boldsymbol{n}$). The parameter $\boldsymbol{g(n)}$ is solvent dependent and can be calculated using the refractive index by the following equation.

$$\boldsymbol{g(n) = \frac{3}{2}\left[\frac{n^4-1}{(n^2+2)^2}\right]} \quad (4)$$

The use of these parameters allows the calculation of the ground state and the exited state dipole moments according to the following equation:

$$\boldsymbol{\frac{\mu_e}{\mu_g} = \frac{m_1+m_2}{m_2-m_1}} \quad (5)$$

2.6 Determination of Zeta Potential

The Zeta Potential measurements were performed in a Zeta PALS potential analyzer (Brookhaven, USA) with parallel-plate platinum black electrodes spaced 5 mm apart and a 10 mm path length rectangular organic glass cell. All the samples were measured using a sinusoidal voltage of 80 V with a frequency of 3 Hz. This measure was determined in solutions containing protein concentrations (BSA and HSA) in a range of 0-3.5 μM and a 2 μM concentration of each dye. For each sample, a total of three values were automatically given by the instrument, which were then averaged to give the final value and the standard deviation.

2.7 Protein assays

In order to investigate protein-dye interactions the dye solutions were prepared in DMF (due to the high insolubility in aqueous medium) and then diluted in PBS buffer. To this solution, the protein stock solution was added and incubated for 1 hour under stirring, at r.t.. In these experiments the dyes concentrations were maintained (2 μM) and the proteins concentrations ranges from 0-3.5 μM. The fluorescence intensity of the final solutions was measured using a λ_{exc}= 580 nm, excitation slit of 10 nm and emission slit of 20 nm.

2.8. Binding parameters determination

The dissociation ($\boldsymbol{K_D}$) and binding ($\boldsymbol{K_B}$) constant values can give an idea about the strength of binding and thereby throws some light on the mode of binding. The apparent dissociation constant ($\boldsymbol{K_D}$) and the Hill's coefficient ($\boldsymbol{n}$) of protein/dye system can be estimated by Hill's Plot using the data from fluorescence protein assays, by the following equation [37]:

$$\boldsymbol{log}\left(\frac{\boldsymbol{Q}}{\boldsymbol{1-Q}}\right) = \boldsymbol{log}\, \boldsymbol{K_D} + \boldsymbol{n log}[\boldsymbol{P}] \qquad (6)$$

where $\boldsymbol{Q} = \frac{\boldsymbol{F}}{\boldsymbol{F_{max}}}$ and [*P*] is the protein (BSA or HSA) concentration.

The values of $\boldsymbol{K_D}$ were obtained from the intercept of the plot of $\boldsymbol{log}\left(\frac{\boldsymbol{Q}}{\boldsymbol{1-Q}}\right)$ *vs* $\boldsymbol{log}[\boldsymbol{P}]$.

The binding constants can be obtained using the assays of protein/dye interaction data through the modified Benesi-Hildebrand equation 7 [38]:

$$\frac{\boldsymbol{1}}{\boldsymbol{F_x - F_0}} = \frac{\boldsymbol{1}}{\boldsymbol{F_\infty - F_0}} + \frac{\boldsymbol{1}}{\boldsymbol{K_B(F_\infty - F_0)}}\,\frac{\boldsymbol{1}}{[\boldsymbol{P}]} \qquad (7)$$

where $\boldsymbol{F_0}$, $\boldsymbol{F_x}$ and $\boldsymbol{F_\infty}$ are the fluorescence intensity in the absence of protein, at an intermediate concentration of protein and at a concentration for complete interaction, respectively; $\boldsymbol{K_B}$ is the binding constant and $[\boldsymbol{P}]$ is the protein (BSA or HSA) concentration. We obtained the value of binding constant plotting a graph of $\frac{\boldsymbol{1}}{\boldsymbol{F_x - F_0}}$ *vs* $[\boldsymbol{P}]^{\boldsymbol{-1}}$.

2.9. Determination of binding site

The determination of the binding sites of the synthesized dyes to the tested proteins was performed using a method already described by Luo *et al.* [4]. Assays were carried out with the different synthesized dyes at a concentration of 2µM, with BSA and HSA at a concentration of 3 µM and with different concentrations of warfarin and ibuprofen (0-100µM).

2.10 Determination of detection limit (DL) and quantification limit (QL)

The detection limit (DL) and the quantification limit (QL) are important parameters in the validation of the method. These parameters were calculated using a calibration curve obtained from the plot of maximum fluorescence intensity as a function of the protein concentration and then we applied the follow equation formulas:

$$\boldsymbol{DL} = \frac{\mathbf{3.3}\boldsymbol{xS.D.}}{\boldsymbol{k}} \quad (8)$$

$$\boldsymbol{QL} = \frac{\mathbf{10}\boldsymbol{xS.D.}}{\boldsymbol{k}} \quad (9)$$

where $\boldsymbol{S.D.}$ is the standard deviation of blank and $\boldsymbol{k}$ is the slope of the curve equation [39].

2.11 Determination of complex dye-protein lifetimes

Lifetime data were obtained using the maximum excitation and emission of each dye at room temperature using frequency domain interrogation. For each case an appropriate wavelength LED was used to excite the sample by direct irradiation. The luminescence emission was guided by a 600-m Y fiber coupler. Luminescence was collected by the same optical fiber and lead to detection by a variable gain amplified silicon photodetector (PDA36A from Thorlabs, Inc.) set at 30 dB amplification and 785 kHz bandwidth. The signal obtained by the detector was fed into a lock-in amplifier (SR844 from SRS) where it was compared with a reference signal from the modulation source. The lifetime study was performed for individual dyes and for the complex dye-proteins. For the last it was used the protein concentration ranged from 0-3.5 µM. When a two-exponential decay was obtained the medium lifetime was calculated using the following expression: $\boldsymbol{\tau_m} =$

$f_1\tau_1 + f_2\tau_2$ where f_1 and f_2 are the fractional intensities and τ_1 and τ_2 represent the obtained lifetimes [40].

3. Results and discussion

3.1. Synthesis of squaraine dyes

The synthesis of the squaraine dyes is presented in Scheme 1. As far as the author's knowledge, synthesis and spectroscopic characterization of squaraine dyes **8b** and **8c** are being presented here for the first time. Indolenine-based barbiturate squaraine dyes with different barbituric acid derivatives, such as thiobarbituric acid (**8b**) and 1,3-diphenyl-2-thiobarbituric acid (**8c**) positionated on the four-membered central ring were synthesized by a multistep reaction (Scheme 1). Dye **8a**, although already reported in a recent work published by some of us [23], has never been evaluated for its potential use as a fluorescent probe for proteins detection.

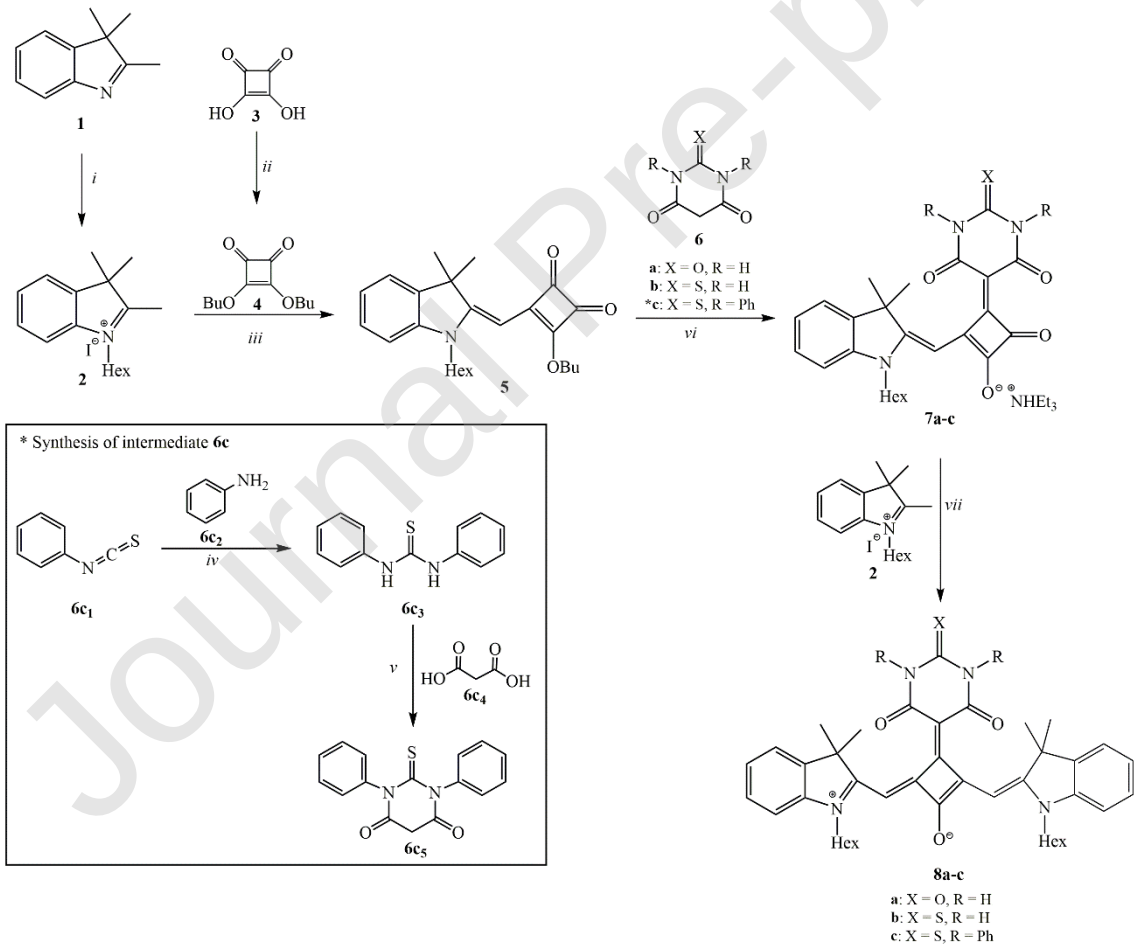

Scheme 1: Schematic representation of the barbiturate squaraine dyes **8a-c** synthesis. Conditions: i) acetonitrile, reflux for 5 days; ii) *n*-butanol, reflux for 4h; iii) EtOH/Et_3N, r.t., overnight; iv) CH_2Cl_2, r.t.

for 3h; v) acetyl chloride, 60°C, 1h; vi) EtOH/Et_3N, reflux, vii) *n*-butanol/ toluene (1:1, v/v), Dean-Stark apparatus.

The barbiturate dyes were synthetized using a similar procedure previously described [33], e.g., the squaric acid (**3**) was refluxed with *n*-butanol, resulting the dibutylsquarate (**4**), that reacted with the quaternary ammonium salt (**2**), which was obtained through the alkylation of 2,3,3-trimethylindolenine (**1**) with an excess of iodohexane, to afford the monosubstituted intermediate **5**. Afterwards, the semisquaraines **7a-c** were obtained upon reaction of the monosubstituted intermediate **5** with barbituric acid (**6a**) or a derivative thereof (**6b** or **c**), and were used in the next reaction without further purification. Finally, the desired barbiturate squaraine dyes **8a-c** were obtained through a base-catalyzed condensation reaction between the respective semisquaraine intermediate **7a-c** and the quaternary ammonium salt **2** in a *n*-butanol/toluene (1:1 v/v) mixture using a Dean-Stark apparatus.

Although barbituric (**6a**) and thiobarbituric acid (**6b**) were used as commercially available, 1,3-diphenyl-2-thiobarbituric acid (**6c**) was obtained by a two-step methodology already described in the literature [32] (Scheme 1, highlighted box). This barbituric acid derivative was obtained by the reaction between the 1,3-diphenylthiourea (**$6c_3$**), which was achieved by the reaction of phenylisothiocyanate (**$6c_1$**) with aniline (**$6c_2$**) in dichloromethane, and malonic acid (**$6c_4$**), in the presence of acetyl chloride.

The structures of synthetized dyes were confirmed by standard spectroscopy methods, namely ^{1}H NMR, ^{13}C NMR, IR and HRMS spectrometry. The carbon atoms attributions were based in DEPT 135 spectra (Fig S1-11 Supplementary Data),

3.2. Photophysical properties of the synthetized dyes

The photophysical properties were studied in organic solvents with different polarities (Table 1). The absorption and emission spectra for the three synthetized dyes in the different solvents are shown in Fig. 1 a-f. As it is possible to see from the figure analysis both absorbance and fluorescence emission are solvent sensitive. Moreover, the observed shift in each solvent is different according to the dye.

Table 1. Photophysical results from UV-VIS/NIR absorption and fluorescence emission of synthesized dyes (**8a-c**) in different solvents.

Dyes	Solvent	λ_{abs} (nm)	λ_{em} (nm)*	Ɛ (M^{-1}. cm^{-1})	Stokes shift (nm)	ϕ_F (%)
8a	PBS	650	708	4.31×10^4	58	-
	MeOH	632	653	9.74×10^4	21	-
	DMF	658	681	1.35×10^5	23	4.8
	$CHCl_3$	644	663	1.04×10^5	19	-
8b	PBS	645	700	5.76×10^4	55	-
	MeOH	630	654	1.30×10^5	24	-
	DMF	652	675	1.47×10^5	23	5.6
	$CHCl_3$	641	661	1.54×10^6	20	-
8c	PBS	650	708	6.61×10^4	58	-
	MeOH	630	653	1.55×10^5	23	-
	DMF	647	673	1.46×10^5	26	8.1
	$CHCl_3$	644	663	1.84×10^5	19	-

* λ_{exc} 580 nm, excitation and emission slits 10 nm.

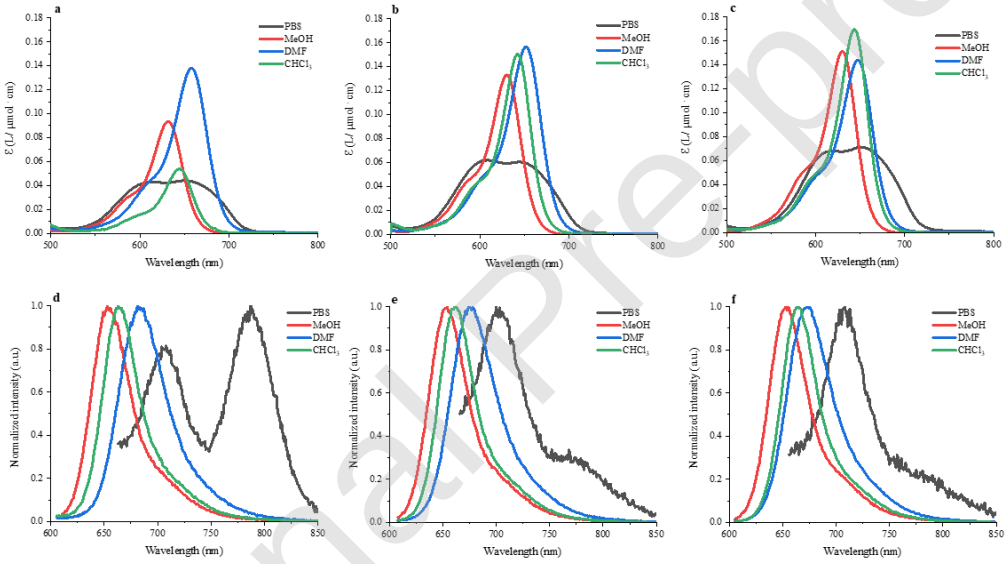

Fig. 1. Absortion spectra (a-c, corresponding to compound **8a-c**, respectively) and normalized emission spectra (d-f, corresponding to compound **8a-c**, respectively) of synthetized dyes in four different solvents. The fluorescent intensities in PBS are practically not measurable (FI = 13 and 16 for dye **8a**; FI = 14 for dye **8b** and FI = 12 for dye **8c**)

It is possible to perform a deconvolution of the absorption peak and obtain two distinct spectral signals one at greater relative wavelength to the monomer band, and other that can be attributed to H-aggregates at a shorter wavelength [41, 42] (absorption band shifted hypsochromic) closely followed by the monomer band (Fig. S12, Supplementary Data). The monomer band is sharp and strong for all dyes, which is consistent to the typical

optical transitions associated with the high delocalization of the π-system [15]. The maximum emission wavelength shift observed in the different solvents is an indication that the dyes are solvatochromic. Each dye had a distinct behavior in the solvents that needs to be further analyzed according to their molecular structure. Both **8a** and **8b** have electron withdrawing ring substituents, the carbonyl and sulfur groups, nonetheless they exhibit some relevant optoelectronic differences since oxygen electronegativity is superior. Indeed, when considering the maximum wavelength shift between dyes absorption and emission in the different solvents it is possible to see that **8a** has a more pronounced wavelength shift in the absorption peak from methanol to DMF (26 nm) than the emission (18 nm). On the other hand and, considering the same solvents, in **8b**, even though it seems to have the same trend, the shifts are too close to be distinguished (22 nm and 21 nm, respectively), probably due to the stability that the ring substituents provide to the dye in the ground state. Indeed, when the absorption peak is more affected than the emission it is possible to say that the ground state energy distribution of the dye is affected by the solvents, and this is most probably related to the polar nature of the dye in this state [43]. On the other hand, **8c** has an electron withdrawing sulfur group and a phenyl group, which in this case, should act as an electron donating substituent. The electron donating ability of the phenyl group is superior than the one obtained by hydrogen substituents (**8a** and **b**), in this sense the electrons π mobility in the excited state should be higher and the dye is less polar in the ground state. In this case the spectral shift in the absorption (17 nm) is less to the emission (20 nm), which provides further evidence that the ground state energy is not particularly affected by the solvents. In order to confirm the influence that the absorbed photon has on the charge's redistribution and its consequence on the conformational change of the excited state, the dipole moment of the ground and excited state were calculated according to the solvatochromic method described by Koutek [44]. This method is based on the dyes absorption and emission spectral shift in different polarity solvents. The reason between the dipole moments of the excited (μe) and ground-state (μg) (Table S1, Supplementary Data) indicates that in all the synthetized dyes the dipole moment of the excited state is higher than in the ground state. Moreover, this reason has a descending trend from **8a** to **8c** (0.5; 0.19; 0.089, respectively). In such cases, the relaxed excited state S_1 is energetically stabilized relative to the ground state S_0 and a significant red shift of the fluorescence will be observed [36].

3.3 Zeta potential of the dyes in the presence of BSA and HSA

It is fairly known that common squaraine dyes forms aggregates in water that quenches their fluorescence and act as a major shortcoming when it is intended the development of sensitive probes for biological molecules [15]. The dyes here described where chemically engineered with the intent to try to overcome this drawback. Before we start with interaction tests between dye and proteins and, in order to better access the stability of the compounds in PBS, a zeta potential assay was developed where each dye was diluted in PBS and then placed in contact with increasing amounts of the studied proteins: BSA and HSA.

The results are present in Figure 2a, b and shows that even before the protein addition all

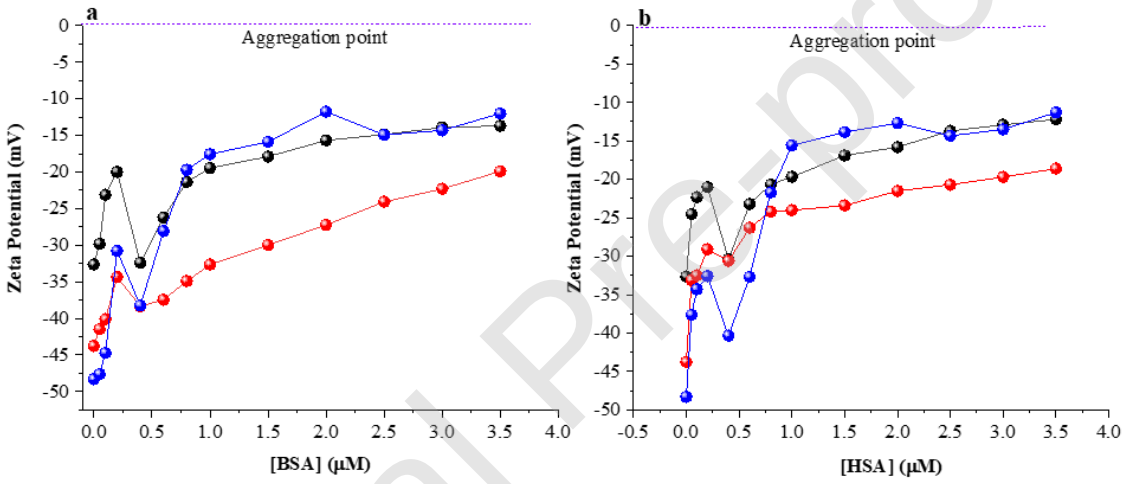

Fig. 2. Zeta potential profile of the three squaraine dyes (**8a** (black), **8b** (red) and **8c** (blue)) in the presence of BSA (a) and HSA (b) in a concentration range of 0-3.5 µM. (The blue dotted line was placed to highlight the aggregation point).

dyes where stable in PBS presenting negative zeta potential values (-33 mV, -48 mV, -44 mV, for **8a-c**, respectively). It was expected that they all exhibit different zeta potential values in PBS, since they have distinct substituents that exert a unique effect on the molecule overall charge distribution. What is interesting to notice is that depict the PBS dissolution they are all far from the aggregation zone (close to 0 mV), thereby demonstrating a higher stability in this common biological buffer than the existing squaraine dyes reported in literature [43].

3.4. Dye-protein association

The non-fluorescent aggregates typical of the squaraine dyes in PBS solutions are often described in the literature [2, 6, 43, 45]. However, reports of their fluorescence in this medium are quite scarce [43]. The synthetized dyes here described also exhibit non-fluorescent aggregates in PBS prior to protein addition (Fig. 3a-c). Upon the addition of BSA (Fig. 3a-c) or HSA (Fig. 4a-c) the complex dye-proteins emit at about 650nm and the emission intensity is directly proportional to the concentration of protein used. It is also interesting to notice that the new adduct dye/protein has a fluorescence intensity 35% higher with BSA than HSA.

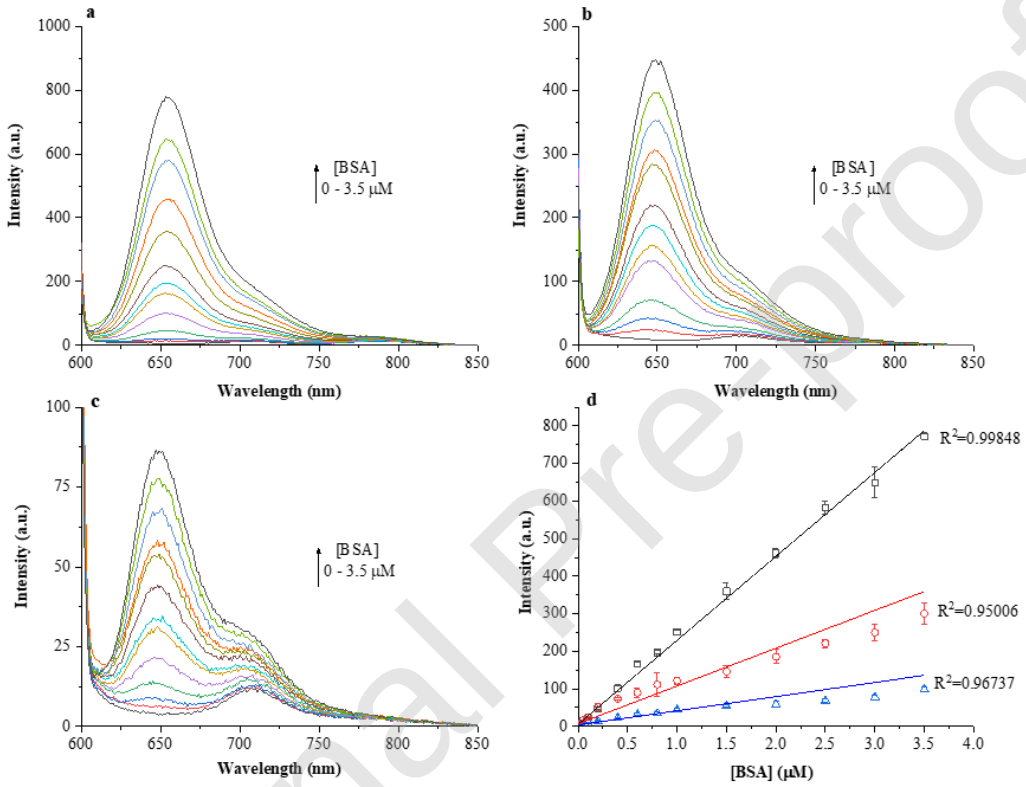

Fig. 3. Fluorescence emission spectra of compounds **8a** (a), **8b** (b) and **8c** (c) in PBS with varied BSA concentrations (0-3.5 µM) for a fixed dye concentration of 2 µM. (d) Maximum fluorescence emission intensity of dyes (**8a** (black), **8b** (red), **8c** (blue)) as a function of BSA concentration in PBS.

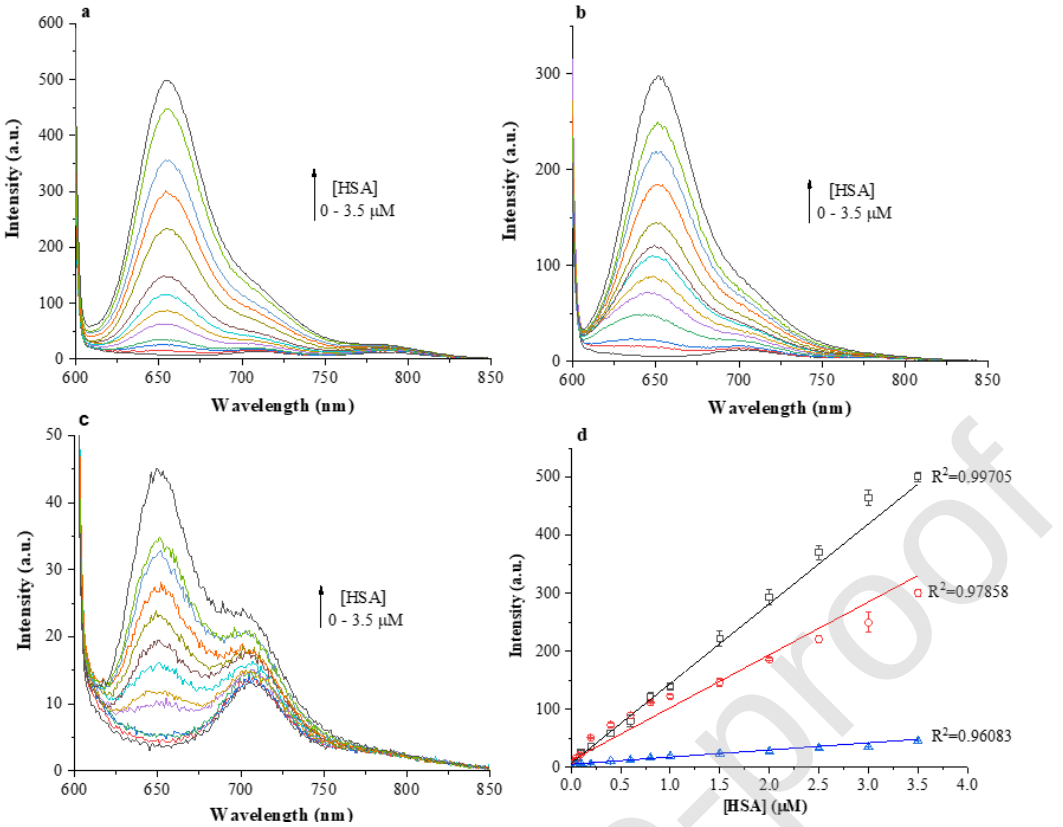

Fig. 4. Fluorescence emission spectra of compounds **8a** (a), **8b** (b) and **8c** (c) in PBS with varied HSA concentrations (0-3.5 µM) for a fixed dye concentration of 2 µM. (d) Maximum fluorescence emission intensity of dyes (**8a** (black), **8b** (red), **8c** (blue)) as a function of HSA concentration in PBS.

In order to better understand the binding mechanism between the synthetized squaraine dyes and the proteins the Hill's plot was analyzed (Fig. S13 a, b, Supplementary Data). Its possible to see that for BSA all dyes exhibit a linear trend, that allowed the determination of the Hills coefficient (n) and the apparent dissociation constant (K_D) (Table 2). According to the obtained results it is possible to say that the interaction between the dyes and BSA is governed by a cooperative mechanism, which is the most common process underlying a large range of biochemical and physiological processes [36, 46]. Moreover, the apparent dissociation constant values provide information on the dye concentration that saturates 50% of the protein binding sites. Considering the data on Table 2, the dye that saturates the protein binding sites at the lowest concentration is **8a**. On the other hand it is possible to add a 55% higher concentration of **8c** (compared to **8a**) to obtain the same saturation of the protein binding sites. It is also interesting to notice that both **8a** and **8c** exhibit a positive cooperativity (n>1) and that **8b** system has a negative cooperativity (n<1) [47], e.g, when dyes **8a** and **8c** bind to BSA in one of its

binding sites, the other binding site are affected by this change. This is also quite visible in the Zeta potential plot (Fig. 2 a, b), where there is a change in the protein conformation that affects the overall surface charge at a similar dye concentration (0.4 μM) for **8a** and **8c**. This phenomenon is less pronounced for **8b**, which is consistent with negative cooperativity where there is a decrease in the binding affinity once the dye bounds to one of the sites [47].

Table 2- Parameters obtained from the Hill's Plot.

Dyes	Hill's Coefficient (*n*)	$K_{D\ (\mu M)}$	R^2
8a	1.29±0.07	0.628±0.04	0.97374
8b	0.892±0.06	0.827±0.04	0.95761
8c	1.05±0.08	1.14±0.05	0.95284

Even though the two studied proteins, BSA and HSA, are quite similar, indeed the main difference in their composition is that HSA has only one tryptophan residue, rather than BSA that has two [45, 47], their interaction with the synthetized dyes is quite different (Fig. S13 a,b, Supplementary Data). The Hill's plots for the assays with HSA exhibits a polynomial fit with n=3. This deviation from the typical linear trend of this plot is consistent with the fact that for HSA the binding mechanism cannot be described as cooperative. This deviation from linearity has been described by Adair [47, 48] that hypothesized that cooperativity is dye saturation dependent and, as such, it is possible to have polynomial fits when the cooperativity is not 1:1 proportion.

The binding constants values further supported the obtained data considering the binding mechanism between the dyes and the proteins. According to the obtained data (Fig. 5a, b) the binding constants are higher for HSA (K_B=9.97x10^5 M; 7.32x10^5 M; 1.27x10^6 M for **8a-c**, respectively) than BSA (K_B=3.60x10^5 M; 6.21x10^5 M; 4.44x10^5 M, for **8a-c**, respectively) which is an indication that the dyes have better chemical/structural affinity towards HSA than BSA. Nonetheless, with the exception of compound **8c** with HSA, the binding constants are all on the same order of magnitude (≈10^5 M). This order of magnitude is consistent with an intercalative binding, that seems feasible considering the dyes π system [38]. Moreover, the parabolic fitting observed for both BSA and HSA with all dyes (Fig. 5a, b) which is an indication of a 1:2 complexation between the dye and the protein [6].

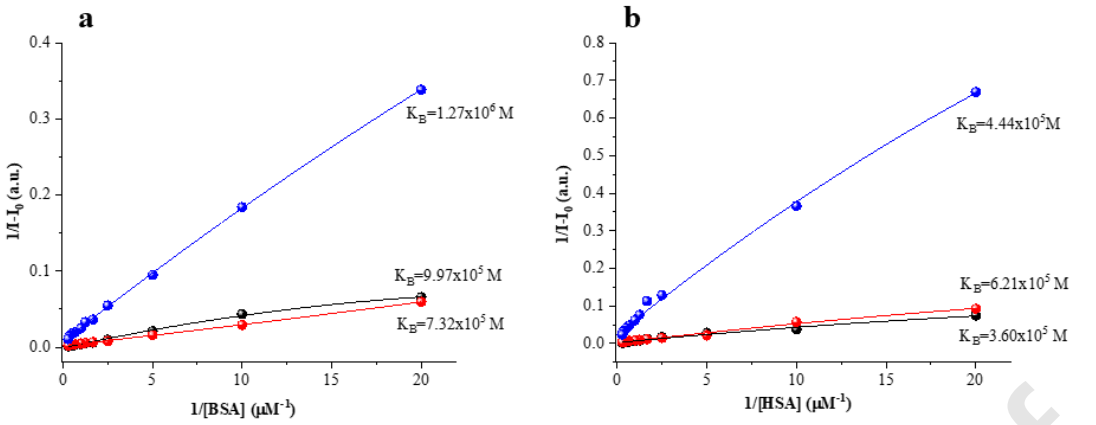

Fig. 5. Benesi-Hildebrand plots for the binding of squaraine dyes (**8a** (black),**8b** (red),**8c** (blue)) to BSA (a) and HSA (b).

The comparison of the obtained binding constants in between dyes, makes it is possible to observe that **8c** has more affinity towards HSA than the other two dyes. This maybe related to two different and concomitant factors. The phenyl substituent provides a molecular stucture more rigid than in the other dyes, but is also confers an hydrophobic nature that can better interact with the hidrophobic moety of both proteins [36].

In order to acquire insight knowledge of the binding site affinity of the dyes for the two proteins, displacement experiments were performed using warfarin and ibuprofen. It is known that warfarin has a high affinity towards binding site I of both proteins and ibuprofen to binding site II [49, 50]. Taking this into account an experiment was designed to understand to which binding site the dyes have preference for. The results demonstrate that the synthesized compounds behave differently depending on the protein used. In the case of BSA (Fig.6a-c), in warfarin assays, there is a gradual increase in the percentage of inhibition for compounds **8a** and **8c**, with a rate of 24% and 38% respectively for the 100 μM concentration of warfarin. For compound **8b** only when the highest concentration of warfarin is used, there is a slight increase in the rate of inhibition (8%). When ibuprofen is used, compound **8a** has an increased inhibition rate, with the opposite effect for compounds **8b** and **8c**. These results suggest that compound **8a** binds to both BSA sites while compound **8b** and **8c** binds only to site I.

In the assays with HSA (Fig. 6d-f) an increase in the % inhibition is observed for all the dyes, with the addition of warfarin and ibuprofen. Upon addition of 100 µM of warfarin the fluorescence of the complex dye-protein was inhibited by 39%, 26% and 32% for **8a**, **8b** and **8c**, respectively. For a concentration of 100 µM of ibuprofen the inhibition rate is 57%, 38% and 45% for **8a**, **8b** and **8c**, respectively. These results lead to the conclusion that all dyes bind to both HSA binding sites. Since the dyes demonstrated the ability to bind to both sites, an experiment was carried out, where there was a simultaneous blocking of the sites, using warfarin and ibuprofen at 50 µM. It is possible to observe that blocking the two sites leads to more pronounced decrease in the fluorescence intensity than when blocking only one binding site. For compound **8a**, with HSA, there is an inhibition rate of 66%, for **8b** 54% and for compound **8c** 42%. It is interesting to notice that despite the use of both blocking agents in a concentration much higher (100 µM) than the one used for the dyes (2 µM), the fluorescence emission is still verified. This is an indication that not only the synthetized dyes can bind to both sites, but also that their binding affinity is higher than the inhibitors usually used to block the sites.

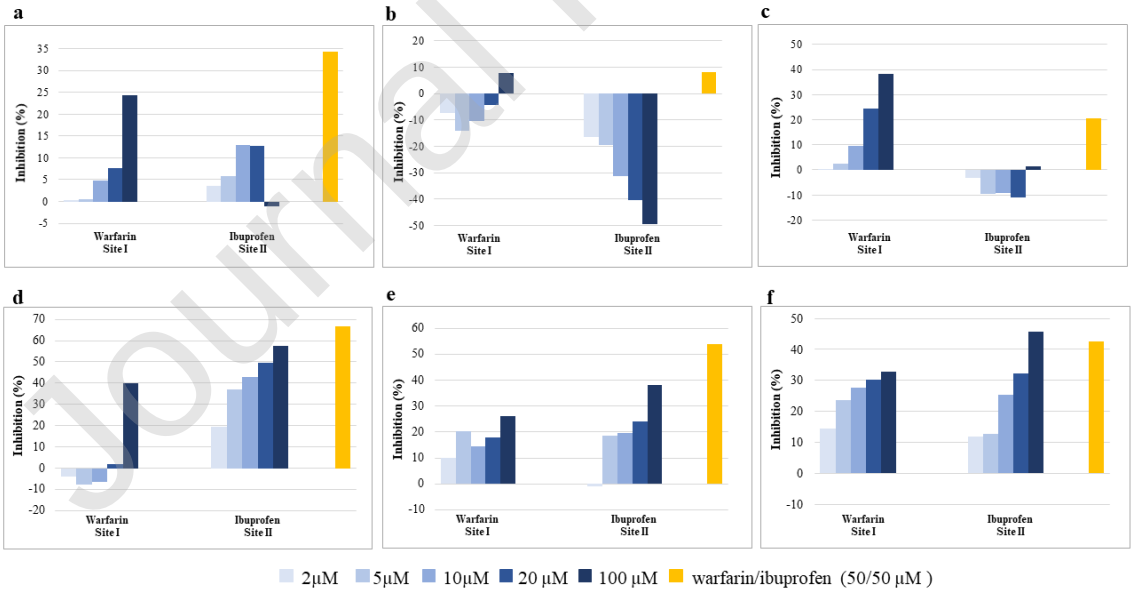

Fig. 6. Inhibition rate of fluorescence intensity for the dye/BSA complex (a-c, corresponding respectively to compound **8a-c**) and dye/HSA complex (d-f, corresponding respectively to compound **8a-c**) by the addition of site-specific markers (warfarin and ibuprofen, 2-100 µM).

3.5. Dye-Protein Sensing System

Despite the different affinities towards the two used proteins all dyes revealed a consistent linear trend between the protein concentration and the maximum fluorescence intensity (Fig. 3d and 4d) that allowed the development of an efficient sensing system in PBS. In Table 3 is possible to see that the DL and QL of both proteins changes with the dye. The dye that has the lowest sensing parameters is **8a**, followed by **8c** and the **8b**. The values here determined are in agreement to the ones previously reported in the literature [43, 51]. Upon the determination of the DL and QL using the fluorescence intensity a similar procedure was performed using the fluorescence lifetime (Table 3). It was found that all the dyes had a mono-exponential decay, which is consistent with these organic dyes [25]. Moreover, **8c** had the lowest lifetime (0.22 ns) when compared to **8a** (0.42 ns) and **8b** (0.34 ns) (Table S2, Supplementary Data), which was to be expected considering the previous calculus of the excited and ground-state dipole moment. On the other hand the complex dye-protein had a two-exponential lifetime decay profile for all dyes in both proteins. Interestingly when in contact with increasing amounts of BSA and HSA, the medium lifetime of all dyes exhibit a similar trend than the one previously observed for fluorescence intensity that could also be linearized in order to obtain the sensing parameters (Fig. 7, Table 3). The **8a** binding to BSA and HSA resulted in a fluorescence lifetime increase of 60% and 54%, respectively. On the other hand, **8b** had an increase of 65% and 59% and **8c** had a boost of 85% and 70%, respectively. This lifetime behavior is consistent to the one observed by Markova *et al.* (2013) [40], where squaraine dyes with different substituents had a distinct lifetime increase when binding to the HSA protein. The DL and QL obtained through the linearization of the lifetime with the protein concentration is slightly lower and has a better sensitivity. This was to be expected, since the fluorescence intensity measurements are more prone to fluctuations that can affect the method precision. Nonetheless they are in the same order of magnitude, further confirming that both techniques effectively reflect the relationship between the proteins concentration and the dyes and can be used indiscriminately.

Table 3. Values of detection limit (DL), quantification limit (QL) and sensitivity of the sensitizing dyes (**8a- c**) with BSA and HSA, calculated using the fluorescence intensity[a] and the medium lifetime[b].

BSA						
Dyes	**DL[a]**	**QL[a]**	**Sensitivity[a]**	**DL[b]**	**QL[b]**	**Sensitivity[b]**

8a	66	199	$2.19x10^5$	42	129	$1.75x10^2$
8b	237	719	$1.20x10^5$	43	133	$1.84x10^2$
8c	187	567	$2.45x10^4$	46	140	$3.67x10^2$
HSA						
Dyes	**DL[a]**	**QL[a]**	**Sensitivity[a]**	**DL[b]**	**QL[b]**	**Sensitivity[b]**
8a	62	199	$1.46x10^5$	52	157	$1.42x10^2$
8b	156	474	$7.77x10^4$	34	104	$1.44x10^2$
8c	152	461	$1.11x10^4$	42	126	$1.50x10^2$

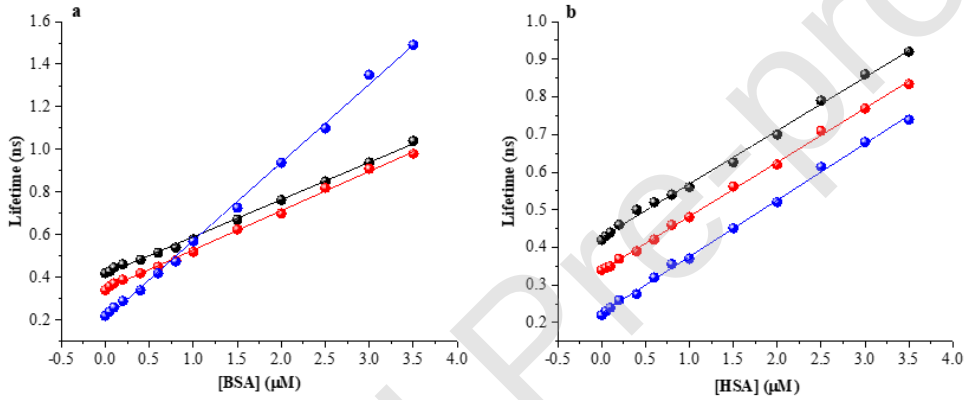

Fig. 7. Fluorescence lifetime of compounds **8a** (black), **8b** (red) and **8c** (blue) in PBS with varied BSA (a) and HSA (b) concentrations (0-3.5 μM) for a fixed dye concentration of 2 μM.

4. Conclusions

Three squaraine dyes containing moieties derived from barbituric acid have been synthesized and their potential as probes for HSA and BSA detection was studied. The dyes have high absorption and emission efficiencies at wavelengths in the Vis/NIR region with high extinction coefficients with an order of magnitude of 10^5 M^{-1} cm^{-1}. The Zeta potential values reveal that the compounds here presented, are quite stable in aqueous media, unlike what has been previously described for other squaraine dyes. The sensing ability of these new dyes was tested towards BSA and HSA proteins. According to the obtained data the synthesized compounds form a complex with the proteins that result in a fluorescence intensity enhancement with increasing protein amounts. Furthermore, the

dye-protein complex is responsible for an up rise of a new Gaussian band in a different wavelength of the dye. Furthermore, the binding constants show that the dyes have a strong interaction and high affinity for both proteins. Regarding the study on the binding sites of dyes to BSA and HSA proteins we can conclude that dye **8a** binds to both BSA sites while dyes **8b** and **8c** binds only to site I, and that all dyes bind to both HSA binding sites. The fluorescence and lifetime behavior of all dyes in contact with the proteins could be linearized, which allowed the determination of DL and QL using both techniques. This feature makes these barbiturate dyes particularly appealing for bioimaging applications using the fluorescence lifetime and two-photon excited fluorescence techniques.

Author Statement

The authors and their involvement on the work are: Vanessa S. D. Gomes performed of the chemical and photochemical experiments and data analysis, contributed with the data discussion and wrote part of the original draft of the manuscript; Helena M.R. Gonçalves performed the photochemical assays, played a role with the data discussion and wrote part the original draft of the manuscript; Renato E. Boto and Paulo Almeida acquired the NMR data and revised the manuscript; Lucinda V. Reis contributed with manuscript writing and revision, with the conception and study design of organic chemistry synthesis, with the analysis and discussion of spectroscopic and photochemical data, and critically revised the manuscript.

Conflicts of interest

The authors declare no conflicts of interest.

Acknowledgments

We acknowledge the European Investment Funds by FEDER/COMPETE/POCI under project POCI-01-0145-FEDER-007491 (CICS-UBI) and Funds by FCT – Portuguese Foundation for Science and Technology, under the projects UID/QUI/UI0616/2019 (CQ-VR). This work was also supported by funds from the Health Sciences Research Center (CICS-UBI) through National Funds by FCT – Foundation for Science and Technology (UID/Multi/00709/2019). H.M.R. Gonçalves was funded by project PTDC/BTM-MAT/30858/2017. FEDER funds through the POCI and by National Funds through FCT - Foundation for Science and Technology under the NORTE-01-0145-FEDER-030858 and by the European Union (FEDER funds through Compete) and National Funds

(FCT/MCTES) through Project UID/QUI/50006/2019. FCT is also acknowledged for the PhD grant UMINHO/BD/43/2016 to Vanessa S. D. Gomes.

References

1. Levitt, D.G. and M.D. Levitt, *Human serum albumin homeostasis: a new look at the roles of synthesis, catabolism, renal and gastrointestinal excretion, and the clinical value of serum albumin measurements.* International journal of general medicine, 2016. **9**: p. 229-255 DOI: https://doi.org/10.2147/IJGM.S102819.
2. Barbero, N., C. Butnarasu, S. Visentin, and C. Barolo, *Squaraine Dyes: Interaction with Bovine Serum Albumin to Investigate Supramolecular Adducts with Aggregation-Induced Emission (AIE) Properties.* Chemistry – An Asian Journal, 2019. **14**(6): p. 896-903 DOI: https://doi.org/10.1002/asia.201900055.
3. Zhang, Y.-Z., Q.-F. Yang, H.-Y. Du, Y.-L. Tang, G.-Z. Xu, and W.-P. Yan, *Spectroscopic Investigation on the Interaction of a Cyanine Dye with Serum Albumins.* Chinese Journal of Chemistry, 2008. **26**(2): p. 397-401 DOI: https://doi.org/10.1002/cjoc.200890076.
4. Luo, Z., B. Liu, K. Zhu, Y. Huang, C. Pan, B. Wang, and L. Wang, *An environment-sensitive fluorescent probe for quantification of human serum albumin: Design, sensing mechanism, and its application in clinical diagnosis of hypoalbuminemia.* Dyes and Pigments, 2018. **152**: p. 60-66 DOI: https://doi.org/10.1016/j.dyepig.2018.01.033.
5. Tong, J., T. Hu, A. Qin, J.Z. Sun, and B.Z. Tang, *Deciphering the binding behaviours of BSA using ionic AIE-active fluorescent probes.* Faraday Discussions, 2017. **196**(0): p. 285-303 DOI: https://doi.org/10.1039/C6FD00165C.
6. Jurek, K., J. Kabatc, and K. Kostrzewska, *Fluorescent amino-substituted squaraine probes for bovine serum albumin.* Coloration Technology, 2017. **133**(2): p. 170-177 DOI: https://doi.org/10.1111/cote.12264.
7. Huang, S., F. Li, C. Liao, B. Zheng, J. Du, and D. Xiao, *A selective and sensitive fluorescent probe for the determination of HSA and trypsin.* Talanta, 2017. **170**: p. 562-568 DOI: https://doi.org/10.1016/j.talanta.2017.01.034.
8. Li, P., Y. Wang, S. Zhang, L. Xu, G. Wang, and J. Cui, *An ultrasensitive rapid-response fluorescent probe for highly selective detection of HSA.* Tetrahedron Letters, 2018. **59**(14): p. 1390-1393 DOI: https://doi.org/10.1016/j.tetlet.2018.02.065.
9. Lee, S., D.-B. Sung, S. Kang, S. Parameswaran, J.-H. Choi, J.S. Lee, and M.S. Han, *Development of Human Serum Albumin Selective Fluorescent Probe Using Thieno[3,2-b]pyridine-5(4H)-one Fluorophore Derivatives.* Sensors (Basel, Switzerland), 2019. **19**(23): p. 5298 DOI: https://doi.org/10.3390/s19235298.
10. Jing, X., C. Xiaozheng, Y. Shuqi, M. Zhaohui, W. Wei, and Z. Wenbin, *Fluorescent Probes for Detection of Protein: From Bench to Bed.* Protein & Peptide Letters, 2018. **25**(6): p. 548-559 DOI: http://dx.doi.org/10.2174/0929866525666180531080624.
11. Liu, C., W. Yang, Q. Gao, J. Du, H. Luo, Y. Liu, and C. Yang, *Differential recognition and quantification of HSA and BSA based on two red-NIR fluorescent probes.* Journal of Luminescence, 2018. **197**: p. 193-199 DOI: <https://doi.org/10.1016/j.jlumin.2018.01.021.

12. Sun, Q., W. Wang, Z. Chen, Y. Yao, W. Zhang, L. Duan, and J. Qian, *A fluorescence turn-on probe for human (bovine) serum albumin based on the hydrolysis of a dioxaborine group promoted by proteins.* Chemical Communications, 2017. **53**(48): p. 6432-6435 DOI: https://doi.org/10.1039/C7CC03587J.
13. Wang, N., C. Xin, Z. Li, G. Zhang, L. Bai, Q. Gong, C. Xu, X. Han, C. Yu, L. Li, and W. Huang, *A reversible fluorescent probe for directly monitoring protein-small molecules interaction utilizing vibration-induced emission.* Dyes and Pigments, 2019. **163**: p. 425-432 DOI: https://doi.org/10.1016/j.dyepig.2018.12.027.
14. Yu, C., X. Li, F. Zeng, F. Zheng, and S. Wu, *Carbon-dot-based ratiometric fluorescent sensor for detecting hydrogen sulfide in aqueous media and inside live cells.* Chemical Communications, 2013. **49**(4): p. 403-405 DOI: https://doi.org/10.1039/C2CC37329G.
15. Lakowicz, J.R., *Topics in Fluorescence Spectroscopy: Principles*. 2006: Springer US.
16. Suzuki, Y. and K. Yokoyama, *Development of Functional Fluorescent Molecular Probes for the Detection of Biological Substances.* Biosensors, 2015. **5**(2): p. 337-363 DOI: https://doi.org/10.3390/bios5020337.
17. Friães, S., A.M. Silva, R.E. Boto, D. Ferreira, J.R. Fernandes, E.B. Souto, P. Almeida, L.F.V. Ferreira, and L.V. Reis, *Synthesis, spectroscopic characterization and biological evaluation of unsymmetrical aminosquarylium cyanine dyes.* Bioorganic & Medicinal Chemistry, 2017. **25**(14): p. 3803-3814 DOI: https://doi.org/10.1016/j.bmc.2017.05.022.
18. Fabian, J., H. Nakazumi, and M. Matsuoka, *Near-infrared absorbing dyes.* Chemical Reviews, 1992. **92**(6): p. 1197-1226 DOI: https://doi.org/10.1021/cr00014a003.
19. Liu, L., J. Chen, Z. Ku, X. Li, and H. Han, *Unsymmetrical squaraine sensitizers containing auxiliary arylamine donor for NIR-harvesting on dye-sensitized solar cell.* Dyes and Pigments, 2014. **106**: p. 128-135 DOI: https://doi.org/10.1016/j.dyepig.2014.03.008.
20. Matsui, M., Y. Haishima, Y. Kubota, K. Funabiki, J. Jin, T.H. Kim, and K. Manseki, *Application of benz[c,d]indolenine-based unsymmetrical squaraine dyes to near-infrared dye-sensitized solar cells.* Dyes and Pigments, 2017. **141**: p. 457-462 DOI: https://doi.org/10.1016/j.dyepig.2017.02.024.
21. Weiss, D.S. and M. Abkowitz, *Organic Photoconductors*, in *Springer Handbook of Electronic and Photonic Materials*, S. Kasap and P. Capper, Editors. 2017, Springer International Publishing: Cham. p. 1-1 DOI: https://doi.org/10.1007/978-3-319-48933-9_37.
22. Law, K.-Y. and F.C. Bailey, *Squaraine chemistry. A new approach to symmetrical and unsymmetrical photoconductive squaraines. Characterization and solid state properties of these materials.* Canadian Journal of Chemistry, 1993. **71**(4): p. 494-505 DOI: https://doi.org/10.1139/v93-070.
23. Lima, E., O. Ferreira, V.S.D. Gomes, A.O. Santos, R.E. Boto, J.R. Fernandes, P. Almeida, S.M. Silvestre, and L.V. Reis, *Synthesis and in vitro evaluation of the antitumoral phototherapeutic potential of squaraine cyanine dyes derived from indolenine.* Dyes and Pigments, 2019. **167**: p. 98-108 DOI: https://doi.org/10.1016/j.dyepig.2019.04.007.
24. Serpe, L., S. Ellena, N. Barbero, F. Foglietta, F. Prandini, M.P. Gallo, R. Levi, C. Barolo, R. Canaparo, and S. Visentin, *Squaraines bearing halogenated moieties as anticancer photosensitizers: Synthesis, characterization and biological evaluation.* European Journal of Medicinal Chemistry, 2016. **113**: p. 187-197 DOI: https://doi.org/10.1016/j.ejmech.2016.02.035.
25. Martins, T.D., M.L. Pacheco, R.E. Boto, P. Almeida, J.P.S. Farinha, and L.V. Reis, *Synthesis, characterization and protein-association of dicyanomethylene squaraine dyes.* Dyes and Pigments, 2017. **147**: p. 120-129 DOI: https://doi.org/10.1016/j.dyepig.2017.07.070.

26. Pisoni, D.S., M.P. de Abreu, C.L. Petzhold, F.S. Rodembusch, and L.F. Campo, *Synthesis, photophysical study and BSA association of water-insoluble squaraine dyes.* Journal of Photochemistry and Photobiology A: Chemistry, 2013. **252**: p. 77-83 DOI: https://doi.org/10.1016/j.jphotochem.2012.11.013.
27. Welder, F., B. Paul, H. Nakazumi, S. Yagi, and C.L. Colyer, *Symmetric and asymmetric squarylium dyes as noncovalent protein labels: a study by fluorimetry and capillary electrophoresis.* Journal of Chromatography B, 2003. **793**(1): p. 93-105 DOI: https://doi.org/10.1016/S1570-0232(03)00367-2.
28. Butnarasu, C., N. Barbero, C. Barolo, and S. Visentin, *Squaraine dyes as fluorescent turn-on sensors for the detection of porcine gastric mucin: A spectroscopic and kinetic study.* Journal of Photochemistry and Photobiology B: Biology, 2020. **205**: p. 111838 DOI: https://doi.org/10.1016/j.jphotobiol.2020.111838.
29. Rongxing Yi, P.D., Fangrui Lin, Binglin Shen, Zhigang Yang, Yihua Zhao, Liang Hong, Ying He, Rui Hu, Jun Song, Junle Qu, and Liwei Liu, *Fluorescence enhancement of small squaraine dye and its two-photon excited fluorescence in long-term near-infrared I&II bioimaging* Optics Express, 2019. **27**(9): p. 12360-12372 DOI: https://doi.org/10.1364/OE.27.012360.
30. Pardal, A.C., S.S. Ramos, P.F. Santos, L.V. Reis, and P. Almeida, *Synthesis and Spectroscopic Characterisation of N-Alkyl Quaternary Ammonium Salts Typical Precursors of Cyanines.* Molecules : A Journal of Synthetic Chemistry and Natural Product Chemistry, 2002. **7**(3): p. 320-330 DOI: https://doi.org/10.3390/70300320.
31. Graça, V.C., M.S. Silva, L.V. Reis, F. Sousa, P. Almeida, J.A. Queiroz, and P.F. Santos, *Ethylenediamine-Derived Chromatographic Ligand to Separate BSA, Lysozyme, and RNase A.* Chromatographia, 2014. **77**(21): p. 1529-1537 DOI: https://doi.org/10.1007/s10337-014-2749-y.
32. Serrano, J.L., P.F. Soeiro, M.A. Reis, R.E.F. Boto, S. Silvestre, and P. Almeida, *Synthesis and process optimization of symmetric and unsymmetric barbiturates C5-coupled with 2,1-benzisoxazoles.* Molecular Diversity, 2019 DOI: https://doi.org/10.1007/s11030-019-09937-4.
33. Tatarets, A.L., I.A. Fedyunyaeva, E. Terpetschnig, and L.D. Patsenker, *Synthesis of novel squaraine dyes and their intermediates.* Dyes and Pigments, 2005. **64**(2): p. 125-134 DOI: https://doi.org/10.1016/j.dyepig.2004.05.003.
34. Shi, Y., C. Li, S. Liu, Z. Liu, J. Zhu, J. Yang, and X. Hu, *Facile synthesis of fluorescent carbon dots for determination of curcumin based on fluorescence resonance energy transfer.* RSC Advances, 2015. **5**(79): p. 64790-64796 DOI: https://doi.org/10.1039/C5RA13404H.
35. Ogunsipe, A., D. Maree, and T. Nyokong, *Solvent effects on the photochemical and fluorescence properties of zinc phthalocyanine derivatives.* Journal of Molecular Structure, 2003. **650**(1): p. 131-140 DOI: https://doi.org/10.1016/S0022-2860(03)00155-8.
36. Patil, N.R., R.M. Melavanki, S.B. Kapatkar, N.H. Ayachit, and J. Saravanan, *Solvent Effect on Absorption and Fluorescence Spectra of Three Biologically Active Carboxamides (C1, C2 and C3). Estimation of Ground and Excited State Dipole Moment from Solvatochromic Method Using Solvent Polarity Parameters.* Journal of Fluorescence, 2011. **21**(3): p. 1213-1222 DOI: https://doi.org/10.1007/s10895-010-0800-4.
37. Małgorzata Maciążek-Jurczyk, J.R.-Z., Anna Sułkowska, *Comparative Analysis of KP-HSA Complex by Spectroscopic Methods.* Acta Physica Polonica A, 2013. **123**(4): p. 673-680 DOI: http://doi.org/10.12693/APhysPolA.123.673.

38. Jana, B., S. Senapati, D. Ghosh, D. Bose, and N. Chattopadhyay, *Spectroscopic Exploration of Mode of Binding of ctDNA with 3-Hydroxyflavone: A Contrast to the Mode of Binding with Flavonoids Having Additional Hydroxyl Groups.* The Journal of Physical Chemistry B, 2012. **116**(1): p. 639-645 DOI: https://doi.org/10.1021/jp2094824.

39. Baird, R.B., A. D.Eaton, and E. W.Rice, *Standard Methods for the Examination of Water and Wastewater (SMWW).* 2017, American Public Health Association, American Water Works Association, Water Environment Federation DOI: https://doi.org/10.2105/SMWW.2882.216.

40. Markova, L.I., E.A. Terpetschnig, and L.D. Patsenker, *Comparison of a series of hydrophilic squaraine and cyanine dyes for use as biological labels.* Dyes and Pigments, 2013. **99**(3): p. 561-570 DOI: https://doi.org/10.1016/j.dyepig.2013.06.022.

41. Bricks, J.L., Y.L. Slominskii, I.D. Panas, and A.P. Demchenko, *Fluorescent J-aggregates of cyanine dyes: basic research and applications review.* Methods and Applications in Fluorescence, 2017. **6**(1): p. 012001 DOI: https://doi.org/10.1088/2050-6120/aa8d0d.

42. Xu, Y., Z. Li, A. Malkovskiy, S. Sun, and Y. Pang, *Aggregation Control of Squaraines and Their Use as Near-Infrared Fluorescent Sensors for Protein.* The Journal of Physical Chemistry B, 2010. **114**(25): p. 8574-8580 DOI: 10.1021/jp1029536.

43. Wang, G., W. Xu, Y. Guo, and N. Fu, *Near-infrared squaraine dye as a selective protein sensor based on self-assembly.* Sensors and Actuators B: Chemical, 2017. **245**: p. 932-937 DOI: https://doi.org/10.1016/j.snb.2017.01.172.

44. Koutek, B., *Dipole moments in excited state. Statistical investigation of methods employing solvatochromism.* 1978 DOI: https://doi.org/10.1135/cccc19782368

45. Jisha, V.S., K.T. Arun, M. Hariharan, and D. Ramaiah, *Site-Selective Binding and Dual Mode Recognition of Serum Albumin by a Squaraine Dye.* Journal of the American Chemical Society, 2006. **128**(18): p. 6024-6025 DOI: https://doi.org/10.1021/ja061301x.

46. Silverstein, T.P., *Principles of Physical Biochemistry (van Holde, Kersal E.; Johnson, W. Curtis; Ho, P. Shing).* Journal of Chemical Education, 1999. **76**(4): p. 474 DOI: https://doi.org/10.1021/ed076p474.1.

47. Stefan, M.I. and N. Le Novère, *Cooperative Binding.* PLOS Computational Biology, 2013. **9**(6): p. e1003106 DOI: https://doi.org/10.1371/journal.pcbi.1003106.

48. Adair, G.S., W.t.c.o.A.V. Bock, and J. H. Field, *The hemoglobin system: VI. The oxygen dissociation curve of hemoglobin.* Journal of Biological Chemistry, 1925. **63**(2): p. 529-545.

49. Nicoletti, F.P., B.D. Howes, M. Fittipaldi, G. Fanali, M. Fasano, P. Ascenzi, and G. Smulevich, *Ibuprofen Induces an Allosteric Conformational Transition in the Heme Complex of Human Serum Albumin with Significant Effects on Heme Ligation.* Journal of the American Chemical Society, 2008. **130**(35): p. 11677-11688 DOI: https://doi.org/10.1021/ja800966t.

50. Fielding, L., S. Rutherford, and D. Fletcher, *Determination of protein–ligand binding affinity by NMR: observations from serum albumin model systems.* Magnetic Resonance in Chemistry, 2005. **43**(6): p. 463-470 DOI: https://doi.org/10.1002/mrc.1574.

51. Choudhury, R., S. Rajeshbhai Patel, and A. Ghosh, *Selective detection of human serum albumin by near infrared emissive fluorophores: Insights into structure-property relationship.* Journal of Photochemistry and Photobiology A: Chemistry, 2019. **376**: p. 100-107 DOI: https://doi.org/10.1016/j.jphotochem.2019.02.038.